Translatome analysis of an NB-LRR immune response identifies important contributors to plant immunity in Arabidopsis

Louis-Valentin Méteignier, Mohamed El Oirdi, Mathias Cohen, Teura Barff, Dominick Matteau, Jean-François Lucier, Sébastien Rodrigue, Pierre-Etienne Jacques, Keiko Yoshioka, Peter Moffett

Journal of Experimental Botany, Vol. 68, No. 9 pp. 2333–2344, 2017
doi:10.1093/jxb/erx078 Advance Access publication 28 March 2017

RESEARCH PAPER

Translatome analysis of an NB-LRR immune response identifies important contributors to plant immunity in Arabidopsis

Louis-Valentin Meteignier[1], Mohamed El Oirdi[1], Mathias Cohen[1], Teura Barff[1], Dominick Matteau[1], Jean-François Lucier[1], Sébastien Rodrigue[1], Pierre-Etienne Jacques[1,2,3], Keiko Yoshioka[4] and Peter Moffett[1,*]

[1] Université de Sherbrooke, Département de Biologie, 2500 Blvd. de l'Université, Sherbrooke, QC, J1K2R1, Canada
[2] Université de Sherbrooke, Département d'informatique, 2500 Blvd. de l'Université, Sherbrooke, QC, J1K2R1, Canada
[3] Centre de recherche du centre hospitalier universitaire de Sherbrooke, Sherbrooke, QC, J1H5N4, Canada
[4] University of Toronto, Department of Cell and Systems Biology, 25 Willcocks St., Toronto, ON, Canada

* Correspondence: peter.moffett@usherbrooke.ca

Received 3 October 2016; Editorial decision 20 February 2017; Accepted 20 February 2017

Editor: Björn Usadel, RWTH Aachen University

Abstract

An important branch of plant immunity involves the recognition of pathogens by nucleotide-binding, leucine-rich repeat (NB-LRR) proteins. However, signaling events downstream of NB-LRR activation are poorly understood. We have analysed the Arabidopsis translatome using ribosome affinity purification and RNA sequencing. Our results show that the translational status of hundreds of transcripts is differentially affected upon activation of the NB-LRR protein RPM1, showing an overall pattern of a switch away from growth-related activities to defense. Among these is the central translational regulator and growth promoter, Target of Rapamycin (TOR) kinase. Suppression of TOR expression leads to increased resistance to pathogens while overexpression of TOR results in increased susceptibility, indicating an important role for translational control in the switch from growth to defense. Furthermore, we show that several additional genes whose mRNAs are translationally regulated, including *BIG*, *CCT2*, and *CIPK5*, are required for both NB-LRR-mediated and basal plant innate immunity, identifying novel actors in plant defense.

Key words: CIPK, ETI, NB-LRR, NLR, plant–microbe interactions, protein translation, PTI, Target of Rapamycin.

Introduction

Plants rely on several surveillance mechanisms to defend against pathogen infection. These include pattern-recognition receptors at the plant cell surface, which detect the presence of pathogen-associated molecular patterns (PAMPs) and induce PAMP-triggered immunity (PTI) (Macho and Zipfel, 2014). To overcome the latter, pathogens deploy effector proteins, many of which interfere with PTI induction (Macho and Zipfel, 2015). Many effectors are delivered to the host cytoplasm, where they can be recognized by specific nucleotide-binding, leucine-rich repeat (NB-LRR) proteins. This recognition leads to the induction of effector-triggered immunity (ETI), which often culminates in a type of cell death known as the hypersensitive response (HR). However, the HR is not required in many cases of ETI (Coll *et al.*, 2011) and although many studies have focused on recognition and activation of NB-LRR proteins, much about ETI signaling remains unknown (Li *et al.*, 2015).

Several studies have shown that ETI and PTI responses trigger qualitatively similar transcriptional responses, but that these responses differ in terms of the timing and amplitude of gene expression changes (Tao *et al.*, 2003; Navarro *et al.*, 2004; Tsuda and Katagiri, 2010). Studies on ETI have shown that a significant modification of the proteome occurs prior to changes to the transcriptome during *Pseudomonas* infection (Jones *et al.*, 2004, 2006). At the same time, activation of the NB-LRR protein N results in a repression of viral transcripts, but does not result in a global repression of host translation (Meteignier *et al.*, 2016). However, the role of translational control of host transcripts during an ETI response has not been extensively studied. Recently, translatome analyses of Arabidopsis in diverse conditions such as heat stress (Yángüez *et al.*, 2013), photomorphogenesis (Liu *et al.*, 2012, 2013), and pollen tube growth (Lin *et al.*, 2014) have been reported. These studies have made use of transgenic Arabidopsis plants expressing a FLAG-tagged ribosomal protein L18 (FLAG-rpL18), which allows for translating ribosome affinity purification (TRAP) (Zanetti *et al.*, 2005). This method results in the isolation of intact, actively translating transcripts, which can then be converted to cDNA and sequenced (TRAP-seq).

To identify candidate genes involved in ETI responses, we have used TRAP-seq to analyse the Arabidopsis translatome upon expression of the *Pseudomonas* effector AvrRpm1, which is recognized by the NB-LRR protein RPM1, from an inducible promoter (Mackey *et al.*, 2002). Our results showed that the ETI translatome showed significant differences from the transcriptome. Many transcripts encoding proteins involved in primary metabolism were down-regulated even though their levels in total RNA did not change, whereas many mRNAs encoding signaling-related proteins showed a status indicating higher translational efficiency, suggesting that ETI results in a highly active translational response (or responses). Furthermore, we tested the requirement for resistance to *Pseudomonas syringae* and *Hyaloperonospora arabidopsidis* for a number of genes whose transcripts showed large changes in translational efficiency after RPM1 activation. This analysis identified several genes required for ETI and PTI, including *CCT2*, *BIG*, and *CIPK5*. At the same time, we have found that Target of Rapamycin (*TOR*) is down-regulated at the translational level upon NB-LRR activation. TOR plays a central role in regulating the translation of growth-related genes (Ren *et al.*, 2012; Xiong *et al.*, 2013; Dobrenel *et al.*, 2016). Disease resistance was enhanced by underexpression of TOR and compromised by TOR overexpression. Our results suggest that TOR is involved in regulating the growth-to-defense switch necessary for immunity, and demonstrate a central role for translational control in coordinating defense responses.

Materials and methods

Plant growth conditions and pathogen infection assays

Arabidopsis thaliana plants were grown in soil under 16 h light/8 h dark cycles at 22 °C. Arabidopsis TOR RNAi and OX transgenic lines, as well as the *rrtf1* mutant (SALK_150614) have been described previously (Deprost *et al.*, 2007; Schweizer *et al.*, 2013). Additional mutant lines were obtained from the Arabidopsis Resource Center (Ohio State University), including *doc1-1* (CS6204), *big* (SALK_1054950C), AT1G60000 (SALK_203629C), *cipk5-1* (SALK_084455C), *cipk5-2* (SALK_063555C), *cct2* (SALK_200207C), AT3G23900 (SALK_015201C), *ops* (SALK_089722C), AT1G07280 (SALK_022732C), AT4G21020 (SALK_151565C), and *pgn* (SALK_034655C). Bacterial inoculations were performed as described by González-Lamothe *et al.* (2012). For *H. arabidopsidis* (*Hpa*) infection assays, plants were grown in Sunshine Mix (http://www.sungro.com/) in a growth chamber at 22 °C, 60% relative humidity (RH), with a 9-h photoperiod. Four-week-old plants were infected with *Hpa* strain Noco2 according to Yoshioka *et al.*, (2006). Plants were infected via spray inoculation and left in a growth chamber with plastic cover at 16 °C, >90% RH for 12 d before disease assessment. Spore counts of 2×10^5 cells ml^{-1} were used for TOR OX, TOR RNAi, *cct2*, and *doc1-1*, and 4.5×10^5 cells ml^{-1} were used for *cipk5* analyses. Trypan Blue staining of seedlings was performed as described by Yoshioka *et al.* (2006).

Ribosome immunopurification and RNA extraction

Cellular extracts from 4-week-old Arabidopsis rosette leaves at 2 h after spraying with DEX (30 μM) or water (mock) were prepared for ribosome immunopurification (IP) followed by RNA purification as previously described (Zanetti *et al.*, 2005; Mustroph *et al.*, 2009). Total RNA from the same samples was purified in parallel. RNA integrity was analysed with a Bioanalyzer using an Agilent RNA 6000 Nano kit following the manufacturer's procedure. For details on quality control analysis see Supplementary Experimental Procedures at *JXB* online.

Sequencing

RNA-seq libraries were prepared as described elsewhere (Carraro *et al.*, 2014). Paired-end sequencing was performed on an Illumina HiSeq 2000 system at the Massachusetts Institute of Technology BioMicro Center (40-bp reads). Total RNA and TRAP libraries were sequenced on two independent sequencing lanes as multiplexed samples as described previously (Carraro *et al.*, 2014). The data discussed in this paper have been deposited in NCBI's Gene Expression Omnibus (Edgar *et al.*, 2002) and are accessible through GEO Series accession number GSE75640 (https://www.ncbi.nlm.nih.gov/geo/query/acc.cgi?acc=GSE75640).

Gene expression analysis

The quality of the raw reads was confirmed using FastQC (v0.10, http://www.bioinformatics.babraham.ac.uk/projects/fastqc/), followed by alignment on the TAIR10 assembly of *A. thaliana* Col-0 genome using TopHat (v2.0.8) (Kim *et al.*, 2013) with default parameters, and with Bowtie 2 (v2.1.0) (Langmead and Salzberg, 2012). Using Samtools (v0.1.18) (Li *et al.*, 2009), reads with a mapq score >10 were kept for subsequent analysis. Cuffdiff (v2.1.1) (Trapnell *et al.*, 2013) was then used with parameters frag-bias-correct, multi-read-correct, and the genome annotations file from NCBI 2013-03-06 to identify 'significant' differentially expressed (RNA-seq) or translated (TRAP-seq) genes using comparisons described in the text. Significance was defined as having a FDR-adjusted *P*-value <0.05 (Benjamini–Hochberg correction for multiple-testing). To conserve visual representation accuracy in scatter-plots of translational efficiency, the null FPKM (fragments per kilobase of exon per million fragments mapped) values of genes with an 'inf' result were replaced by the smallest FPKM value seen for the gene within each comparison, and the Log_2-fold change was recalculated to replace the 'inf' value (see Supplementary Table S5 at *JXB* online).

Gene ontology analysis

The DAVID bioinformatics resource 6.7 (http://david.abcc.ncifcrf.gov) was used to analyse enriched gene ontology (GO) terms and protein domains in corresponding datasets compared to the Arabidopsis background, as described previously (Huang *et al.*, 2009). Genes with Log_2-fold changes ≤–2 or ≥2 were used for this analysis, except for all down-regulated differentially expressed genes.

Results

TRAP enables the purification of high-quality translated mRNAs

We crossed plants with a DEX-inducible AvrRpm1 transgene (Mackey *et al.*, 2002) with a transgenic line constitutively expressing a tagged cytosolic ribosomal protein, FLAG-rpL18, generating the Avr/L18 line, allowing for translating ribosome affinity purification (Zanetti *et al.*, 2005), followed by sequencing (TRAP-seq) (Juntawong *et al.*, 2014) (Fig. 1A). As in the parental DEX-AvrRpm1 plants (Mackey *et al.*, 2002), a strong HR developed 4 h after spraying Avr/L18 plants with DEX (see Supplementary Fig. S1A). We also crossed the FLAG-rpL18 line with a *rpm1/rps2* double-mutant line expressing the DEX-AvrRpm1 transgene, but AvrRpm1 was not inducible by DEX in the progeny, probably due to transgene silencing, as previously reported (Geng and Mackey, 2011). To test the efficacy of the TRAP method, we immunopurified ribosomes with anti-FLAG beads. FLAG-rpL18 co-immunoprecipitated the small sub-unit ribosomal protein S14, except in the presence of EDTA, which chelates the Mg^{2+} required for ribosome subunit association (Supplementary Fig. S1C). RT-PCR analysis of purified ribosomes showed that the chloroplastic *RBCL* transcript is largely depleted from the IP fraction, whereas cytosolic transcripts (*GAPDH*, *MEKK1, WRKY38*) are readily detectable (Supplementary Fig. S1D). Together, these results indicate that TRAP allows for the purification of intact cytosolic ribosomes along with associated mRNAs with little background.

To analyse the defense translatome, we treated Avr/L18 plants with DEX or a mock treatment, followed by purification of total RNA and TRAP analysis at 2 h post-treatment. At this time-point, no visible phenotype is apparent on DEX-treated plants and it is well before the manifestation of any DEX- or AvrRpm1-induced phenotypes, which take days to weeks to appear (Kang *et al.*, 1999; Geng *et al.*, 2016). In parallel, we performed polysome profiling on plants treated the same way. No obvious reduction in total polysome abundance was observed in polysome profiles 2 h after DEX treatment (Fig. 1B), indicating that protein translation was not globally repressed upon NB-LRR activation. As shown by immune-blotting, anti-FLAG TRAP yielded approximately the same quantity of rpL18 at 2 h after DEX or mock treatment (Supplementary Fig. S1E, top panel). Likewise, Bioanalyzer analysis showed very similar amounts of high-quality rRNA, from cytosolic ribosomes only, both after mock and DEX treatment (see Supplementary Fig. S1E). RT-PCR confirmed that the *AvrRpm1* transcript was detectable in ribosome fractions only after DEX treatment, as was the *TBF1* transcript, a marker of the growth-to-defense transition (Pajerowska-Mukhtar *et al.*, 2012). As shown above, chloroplastic *RBCL* transcripts were largely depleted in the IP fraction, whereas *RBCS* mRNAs are equally detectable in the total RNA versus the TRAP RNA fraction (Supplementary Fig. S1E). These samples were then used for the construction of sequencing libraries, in parallel with their total RNA fraction counterparts, followed by library quality assessment and paired-end sequencing (Supplementary Fig. S1E). The two techniques (RNA-seq and TRAP-seq) were conducted in biological triplicates under the two conditions (2 h after DEX or mock treatment) to generate twelve libraries.

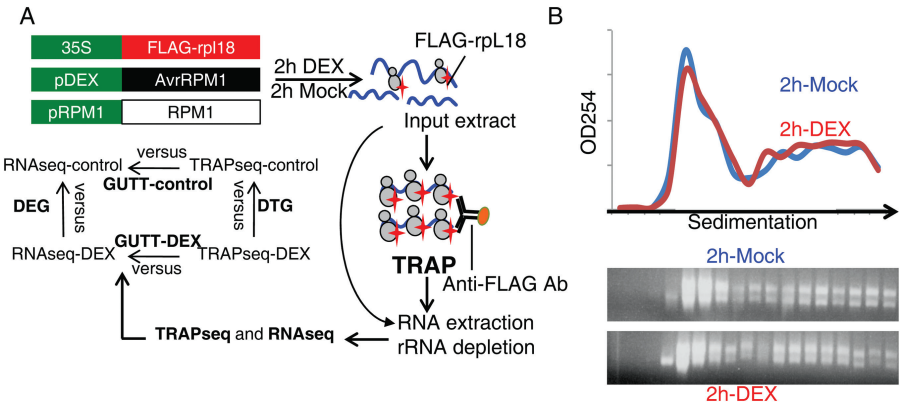

Fig. 1. Experimental design to study the NB-LRR translatome. (A) Schematic diagram of the experimental design. A transgenic Arabidopsis line carrying a DEX-inducible *AvrRpm1* transgene together with a 35S:FLAG-rpL18 transgene, as well as the endogenous *RPM1* gene was generated. Ribosome-bound RNA, isolated using an anti-FLAG antibody, and total RNA was purified 2 h after mock treatment or RPM1 activation by DEX treatment. Immunoprecipitated and total RNAs were then converted to cDNA sequencing libraries to generate TRAP-seq and RNA-seq datasets. Differentially expressed genes (DEGs) and differentially translated genes (DTGs) were identified by comparing DEX versus control from RNA-seq and TRAP-seq data, respectively. Genes showing uncoupled translation and transcription (GUTT) were identified by comparing translational efficiency in each condition. (B) Tissues from mock-treated plants or plants treated with DEX as in (A) were harvested and subjected to polysome profiling and measuring of O.D. 254 absorption of sucrose gradient fractions. The corresponding sucrose fractions were resolved on native 1.2% agarose gels and visualized by ethidium bromide staining. A representative profile from three biological replicates is shown.

Common and contrasting features between the defense translatome and transcriptome

We first assessed the quality of our libraries by looking at the efficiency of rRNA depletion as well as biological reproducibility. For each library, 20–40 million reads were uniquely mapped on the TAIR10 assembly of *Arabidopsis thaliana* Col-0 using TopHat (Trapnell *et al.*, 2009), with a mean rRNA contamination of 5.9% (see Supplementary Fig. S2A, C), and relative gene expression values (FPKM) were obtained using Cufflinks (Trapnell *et al.*, 2010). The average Pearson correlation values between biological replicates for total RNA-seq datasets was 0.85 (Supplementary Fig. S2B), whereas it was above 0.98 for TRAP-seq biological replicates (Fig. S2D). This is consistent with previous reports showing that transcription is inherently more 'noisy' than translation (Keene, 2007; Joshi *et al.*, 2011; Coate *et al.*, 2014). Using Cuffdiff (Trapnell *et al.*, 2013), we identified 1292 differentially expressed genes (DEGs) by comparing the expression levels in mock and DEX conditions from the RNA-seq datasets, of which 25% showed decreased levels after DEX treatment (Fig. 2A, Supplementary Table S1). We also identified 6225 differentially translated genes (DTGs) by comparing the TRA-Pseq datasets from the mock and DEX treatments. Approximately equal numbers of DTGs were

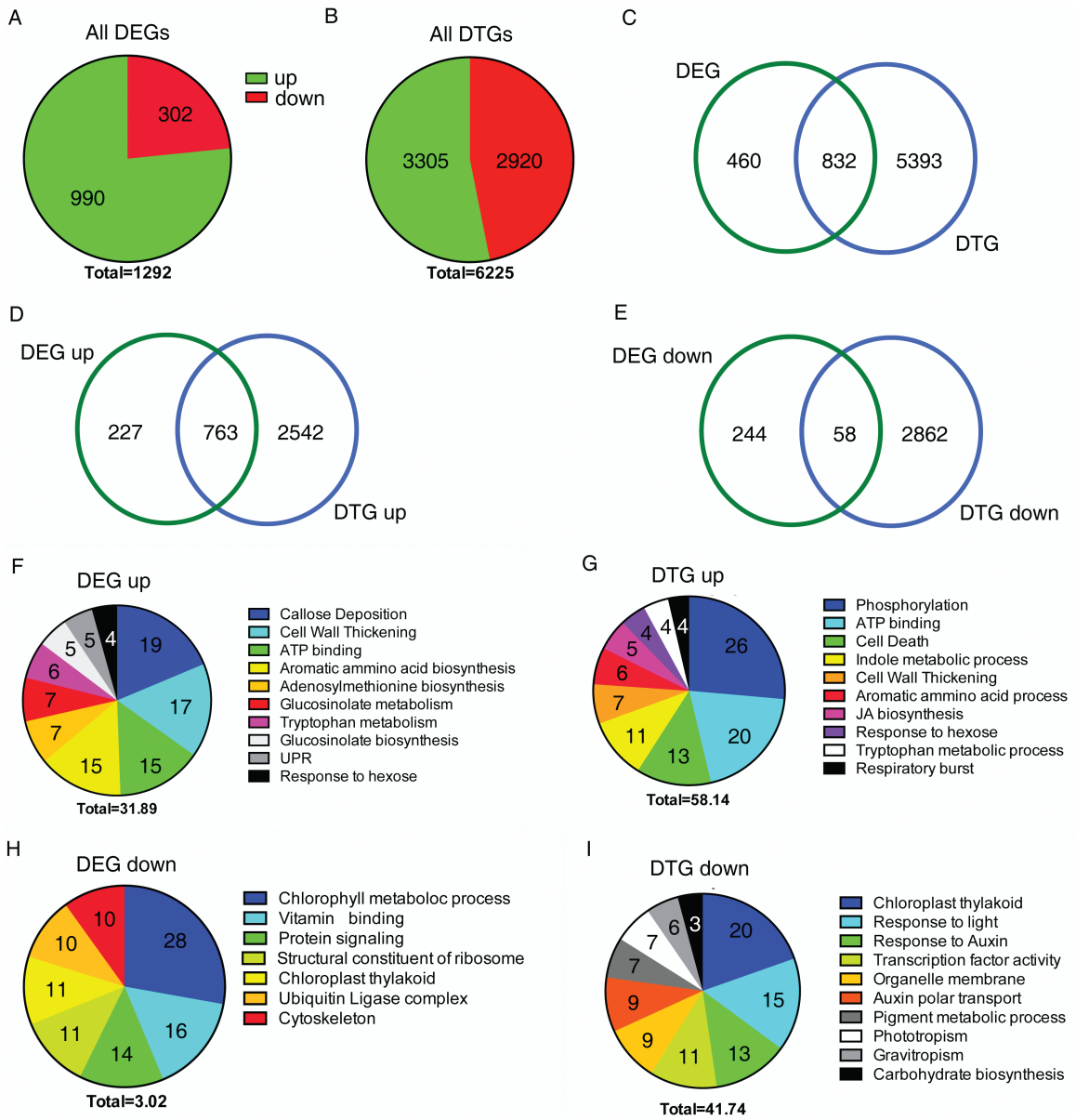

Fig. 2. Analysis of the defense transcriptome and translatome. (A, B) Numbers of DEGs identified from the RNA-seq datasets (A) and DTGs from the TRAP-seq datasets (B), separated into up- (green) and down- (red) regulated genes. (C–E) Venn diagrams showing the overall overlap between the DEGs and DTGs (C), and between the subsets of up-regulated genes (D) and down-regulated genes (E). (F–H) Pie diagrams of the top10 enriched GO terms in the up-regulated DEGs (F) and DTGs (G) datasets, and the down-regulated DEGs (H) and DTGs (I) datasets as resolved by DAVID. The numbers shown at the bottom of the pie diagrams are the sums of the enrichment scores of each GO term indicated in one pie, as calculated by DAVID. Individual GO term percentages relative to the total enrichment score of each pie is indicated for each term.

down- or up-regulated upon NB-LRR activation (Fig. 2B, Supplementary Table S2), and 62% of the DEGs were also identified as DTGs (Fig. 2C). Interestingly, the proportion of DEGs that are also DTGs increased to 77% for up-regulated genes (Fig. 2D), while only 20% of down-regulated DEGs were identified as DTGs (Fig. 2E). This indicates that, in many cases, transcription was uncoupled from translation, particularly for transcriptionally repressed genes. Functional annotation clustering using the DAVID bioinformatics resource revealed that the top 10 enriched GO terms included defense-related processes, including cell wall thickening and secondary metabolism, both at the transcriptional and translational levels (Fig. 2F and G, respectively). At the same time, cell death-related processes appeared in the top10 enriched GO terms only from the DTGs, suggesting a quick induction of HR-related proteins via translational regulation. Consistent with the GO terms, many up-regulated DEGs and DTGs possess TIR domains found in NB-LRR proteins (Supplementary Fig. S2E, F). In contrast to the overlap seen between up-regulated DEGs and DTGs, GO terms enriched in down-regulated genes showed major differences between the two sets of differentially regulated genes. For example, a number of genes belonging to the 'structural constituent of ribosome' GO term were down-regulated at the level of total RNA (RNA-seq DEGs; Fig. 2H, Table S3). However, no genes belonging to this GO term were significantly decreased at the translational level (TRAP-seq DTGs; Fig. 2I; Supplementary Table S3), possibly because certain highly translated mRNAs were not sufficiently turned over in their association with ribosomes within the time-frame of these experiments. GO terms enriched in the down-regulated DTGs largely belonged to primary metabolism and development, including photosynthesis, gravitropism, phototropism, auxin metabolism, and carbohydrate biosynthesis (Fig. 2I; Supplementary Table S3). Interestingly, RPM1 activation also induced a down-regulation of genes encoding proteins involved in carbohydrate biosynthetic process at the translational but not at the transcriptional level, albeit other photosynthesis-related GO terms appeared in the down-regulated DEGs as chlorophyll metabolic process (Supplementary Table S3). Together, these results further indicate that the repression of gene expression correlates poorly at the transcriptional and translational levels, but suggest a rapid growth-to-defense transition based on translational control.

Identification of genes with uncoupled translation and transcription (GUTT) induced by NB-LRR activation

In a theoretical situation in which there is no translational control, all mRNAs should be represented comparably in both the RNA-seq and the TRAP-seq datasets. We used Cuffdiff to identify genes that were either over- or under-represented in the TRAP-seq dataset compared to the RNA-seq dataset. Analysing the control datasets (TRAP-seq versus total; no DEX), we identified 1169 genes showing uncoupled translation and transcription (GUTT), indicating that they were translated either more or less efficiently than the average mRNA. Interestingly, this number was divided by approximately one half (541) 2 h after NB-LRR activation (defense), and only 115 transcripts were common to both control and defense GUTT datasets (Fig. 3A, Supplementary Table S4). This indicates a significant translational reprogramming in host cells upon RPM1 activation. The translational efficiency (TE) of each gene can be represented by the Log_2 ratio of the TRAP-seq FPKM value divided by the RNA-seq FPKM value, as calculated by Cuffdiff, with the expected ratio being 1. Graphic representation of the TE values for the 115 GUTT identified in both control and DEX conditions illustrated a positive correlation (r=0.81, P<0.0001) between control TEs and DEX TEs (Fig. 3B, Supplementary Table S5). That is, most genes that had a positive or negative TE in the absence of defense showed similarly positive or negative TE after NB-LRR activation. However, several genes deviated significantly from the 95% confidence interval boundaries, indicating that their translational status changed significantly after DEX induction. For example, these included genes that had a positive TE under normal conditions, but negative TE upon NB-LRR activation, including *CIPK5* (*CBL-Interacting Protein Kinase 5*) (Fig. 4A), *LBD1* (*LOB Domain-containing protein 1*), and *HBI1* (*Homolog of Bee2 Interacting with IHB1*) (Fig. 3B), the latter having previously been shown to be involved in the plant growth-to-defense switch (Fan *et al.*, 2014; Malinovsky *et al.*, 2014). Conversely, *LEA* (*Late Embryogenesis Abundant*) and *LCR67* (*Low-molecular-weight Cysteine-Rich 67*), encoding a dehydrin and a defensin, respectively, showed negative TEs under normal conditions and positive TEs upon NB-LRR activation (Fig. 3B). At the same time, 426 transcripts showed a TE not significantly different from 0 (FDR<0.05) (which we consider as a normal TE, representative of the average mRNA) under control conditions, but either a positive or negative TE upon NB-LRR activation and are therefore designated as defense-specific GUTTs (Fig. 3A, Supplementary Table S4). For example, *TOR* (*Target of Rapamycin*) showed a normal TE under control conditions, but a significantly negative TE upon NB-LRR activation (Figs 3C and 4B, Table 1, and Supplementary Table S5). Likewise, *PGN* (*Pentatricopeptide repeat protein for Germination on NaCl*), which is required for defense against the necrotroph *Botrytis cinerea* (Laluk *et al.*, 2011), was strongly down-regulated (Fig. 3C, Table 1, and Supplementary Table S5). Conversely, *CCT2* (*Phosphorylcholine Cytidylyltransferase 2*) showed a normal TE under control conditions, but a positive TE upon NB-LRR activation (Figs 3C and 4C, Table 1, and Supplementary Table S5). To definitively attribute TE shifts between control and defense conditions to translational regulation and not to transcriptional effects, we systematically examined the expression data of DEGs and DTGs and compared these results to corresponding gene TEs in both treatments. This process revealed that for 32% of the 1595 GUTT (509 out of the sum of the three groups of GUTT) showing a TE differential between DEX and control, the differential was attributable to TRAP-seq changes but not RNA-seq changes (Supplementary Table S6). In other words, 32% of TE changes upon NB-LRR activation were attributable only to translational regulation. For example, *HBI1* was well

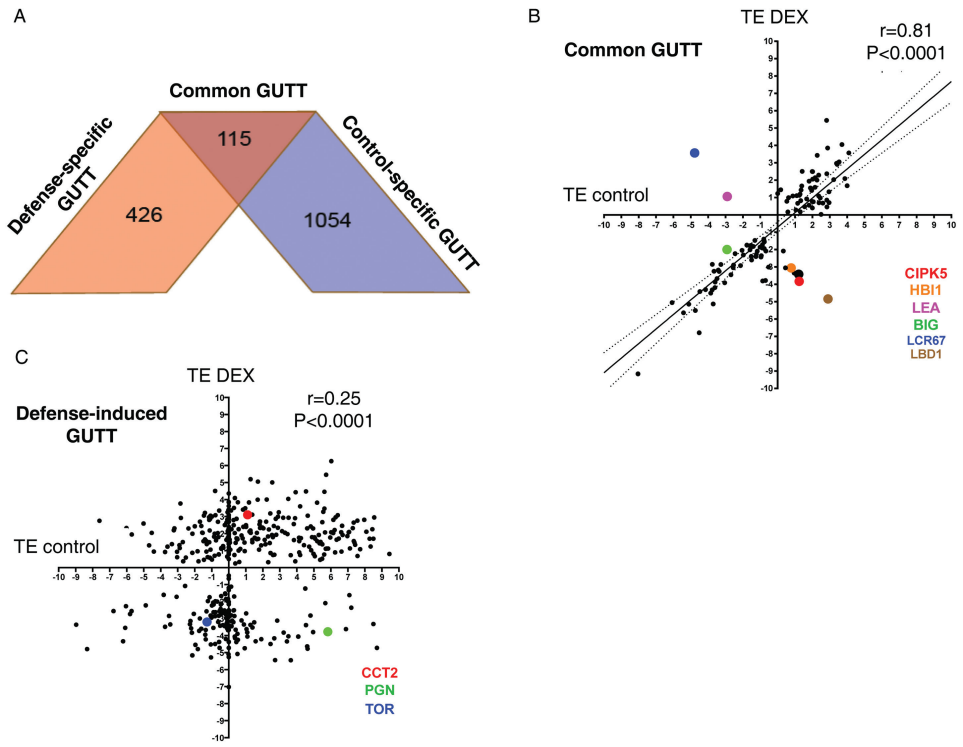

Fig. 3. Identification of translationally controlled genes upon NB-LRR activation. (A) Asymmetric Venn diagram showing the number of genes with uncoupled translation and transcription (GUTT) after DEX treatment (defense) and their overlap with control GUTT (GUTT-common). (B) Scatter-plot of the translational efficiency (TE) [Log_2(FPKM-TRAPseq/FPKM-RNAseq)] in control versus defense conditions for the 115 GUTT-common. The linear regression line (solid black line) is shown together with the 95% confidence interval (dashed black lines). (C) Scatter-plot of the TE in control versus defense conditions for the 426 GUTT-defense. The positions of individual genes of interest are shown as colored dots in (B) and (C).

translated before DEX treatment, with a TE of 0.7 compared to a TE of –3 after DEX treatment. Likewise, the association of *HBI1* transcripts with ribosomes was reduced 38-fold upon DEX treatment (TRAP-seq Log_2-fold change = –5.26) while no significant change was seen at the level of total RNA (RNA-seq). Thus, *HBI1* appeared to be strongly repressed at the translational level upon DEX treatment (Table 1). In contrast, *TBF1* was induced at the total RNA level and at the translational level (see Supplementary Fig. S3). Table 1 lists a number of additional genes of interest that showed a significant alteration of TE upon DEX treatment. Overall, these results suggest that the translational status of many individual transcripts can be affected either positively or negatively upon activation of ETI responses without necessarily involving transcriptional changes.

Validation of candidate genes

To validate the involvement of translational control in defense responses, we tested Arabidopsis mutant lines for altered responses to infection by *Pseudomonas syringae* pv. tomato (*Pst*). We selected genes showing TE differentials during a NB-LRR response without significant transcriptional changes (GUTT-Defense or GUTT-Common; Fig. 3B and 3C; Supplementary Table S6). From these, we prioritized those with the highest TE differentials and for which confirmed homozygous knock-out lines were available from TAIR, including: AT5G10930 (*CIPK5*), AT4G15130 (*CCT2*), AT1G56570 (*PGN*), AT3G02260 (*BIG*), AT1G60000 (unknown RNABP), AT4G21020 (*LEA*), AT3G09070 (*OPS*; *Octopus*), AT3G23900 (unknown RNABP), AT1G07280 (unknown TPR-containing protein), and AT4G34410 (*RRTF1*; *Redox Responsive Transcription Factor 1*). Additionally, we tested the effect of TOR perturbation on plant immunity because TOR is directly involved in translational regulation, and because the translational status of genes involved in carbohydrate anabolism are altered both after NB-LRR activation (Fig. 2F, G, I) and by TOR inhibition (Menand *et al.*, 2002; Ren *et al.*, 2012; Xiong *et al.*, 2013). Null mutants for TOR are not viable, but we obtained a TOR knock-down transgenic line (TOR RNAi) (Menand *et al.*, 2002; Schepetilnikov *et al.*, 2011) as well as a transgenic line that overexpresses TOR (TOR OX) (Deprost *et al.*, 2007).

Mutant Arabidopsis lines were challenged with *Pst* DC3000 (AvrRpm1). Monitoring the number of bacteria at 0 and 3 d post-infiltration (dpi) revealed that the *big* mutant, and to a lesser degree, the *cct2* and *rrtf1* mutant lines allowed more growth of avirulent bacteria, indicating that these genes are required for optimal RPM1-mediated resistance (Fig. 5A). In contrast, in a separate set of experiments, two independent *CIPK5* mutant lines (*cipk5-1* and *cipk5-2*) showed less bacterial growth at 3 dpi (Fig. 5B), suggesting that CIPK5 is a negative regulator of defense. Interestingly, the most closely related homolog of *CIPK5*, *CIPK25*, showed a highly similar TE pattern (5.07 Log_2-fold difference between control and

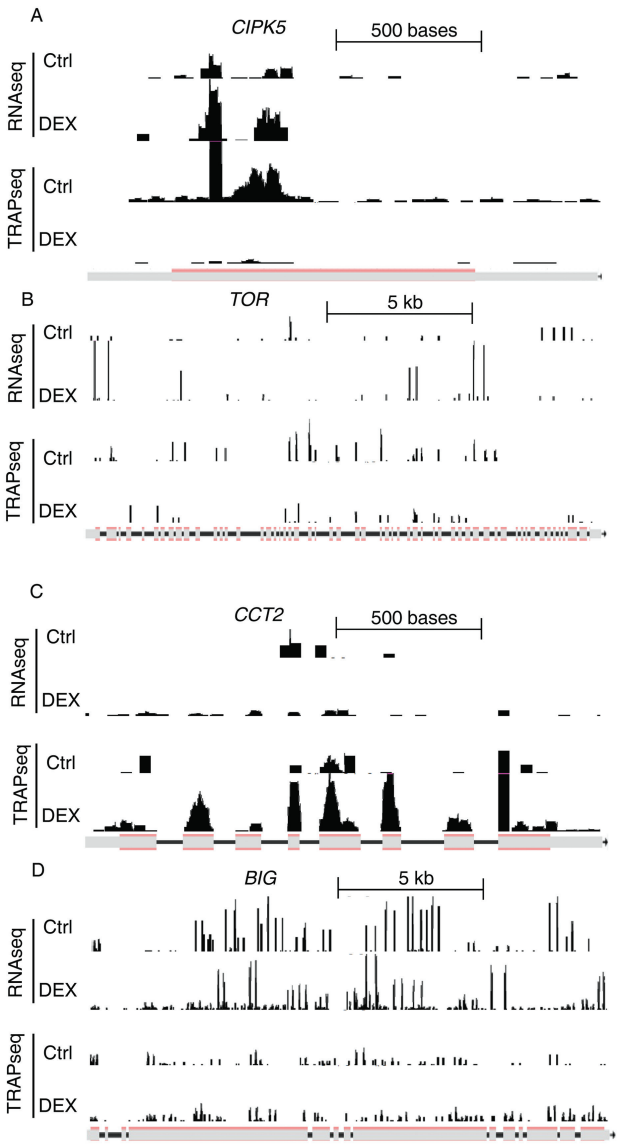

Fig. 4. Visual representation of RNA-seq and TRAP-seq data for individual genes. Raw-read distributions and numbers of hits from the RNA-seq and TRAP-seq datasets were visualized with the UCSC genome browser for the *CIPK5* (A), *BIG* (B), *CCT2* (C), and *TOR* (D) genes. Each panel is representative of the three biological replicates. The *y*-axis maximum is set at 2900 (*CIPK5*), 400 (*BIG*), 600 (*CCT2*), and 400 (*TOR*) fragments.

defense TE) (see Supplementary Table S5). However, infection of a *cipk25* mutant did not result in increased resistance (Fig. 5B). This may be due to a lack of functional redundancy or to the fact that *CIPK25* is expressed at much lower levels compared to *CIPK5* (see Supplementary Table S4). The TOR RNAi line was also more resistant to *Pst* DC3000 (AvrRpm1) (Fig. 5C). Likewise, this line was also more resistant to *Pst* DC3000 (EV) (Fig. 5D). These results suggest that down-regulation of TOR results in a faster and/or more effective disease resistance response. Infection of the TOR OX line with *Pst* DC3000 (EV) or (AvrRpm1), however, did not lead to a significant difference compared to Col-0 (Fig. 5C, D).

For further validation, we tested candidate genes with the most pronounced phenotypes in the *Pst* assay (*cct2*, *big*, and *cipk5*), including an additional point-mutant allele (*doc1-1*) of *BIG* (Gil *et al.*, 2001), as well as the lines with altered TOR expression, using the oomycete pathogen, *Hyaloperonospora arabidopsidis* (*Hpa*) strain Noco2, which is virulent on WT Col-0. Consistent with the results seen with *Pst*, spore counts from infected leaves revealed that the TOR RNAi line was less susceptible to *Hpa* (Fig. 5E). Unlike *Pst*, however, TOR OX plants were significantly more susceptible to *Hpa* (Fig. 5E). Likewise, *cct2* and *big* mutants showed a dramatic increase in susceptibility (Fig. 5F) and *cipk5* mutants showed decreased susceptibility (Fig. 5G). This was also supported by Trypan Blue staining, which clearly showed increased hyphal growth and oospore generation in TOR OX, *cct2*, and *big*, and a decrease in TOR RNAi and *cipk5* plants (Fig. 5H, I).

Although the direct targets of translational control of TOR in plants are unknown, we nonetheless compared our defense transcriptome analysis with transcriptomic data produced from plants in which TOR was pharmacologically inhibited (Ren *et al.*, 2012). Interestingly, up-regulated genes in the transcriptome of TOR-inhibited plants were significantly enriched for 'defense response', 'innate immune response', and other GO terms related to immunity, such as 'response to oxidative stress' and 'secondary metabolites' (see Supplementary Fig. S4A). However, the overlap between up-regulated genes in the transcriptome of TOR-inhibited plants and our transcriptome (total RNA-seq) accounted for only 80 genes (Fig. S4B). Not surprisingly, these 80 genes mainly belong to immune-related GO terms (Fig. S4C), suggesting an overlap between TOR and NB-LRR signaling and partially explaining the resistance phenotypes of plants with altered TOR expression.

Discussion

TRAP-seq using FLAG-rpL18 has been used to identify genes expressed in specific cell types (Reynoso *et al.*, 2015) and related translational profiling methods have been used to characterize plant responses to abiotic stresses (Juntawong and Bailey-Serres, 2012; Yángüez *et al.*, 2013; Juntawong *et al.*, 2014; Vragovic *et al.*, 2015) as well as virus infection (Moeller *et al.*, 2012). We found that defense-induced changes in the translational status of a number of individual transcripts, as defined by ribosome association, was significantly different from what would be predicted from their total abundance. These alterations appeared to be selective as NB-LRR activation did not trigger a global reduction in polysomes (Fig. 1B), as is seen during heat stress (Yángüez *et al.*, 2013), hypoxia (Juntawong *et al.*, 2014), or UV exposure (Meteignier *et al.*, 2016). The reasons for alteration in the relative association of different transcripts with ribosomes could be due to various mechanisms and the TEs calculated for individual mRNAs may not correlate perfectly with translational activity in all cases. Nevertheless, the translational status of a large number of transcripts did change during ETI and we suggest that the TE values obtained are in most cases indicative of their translational status. Other methods, such as ribosome footprinting, can provide additional information on how mRNAs are regulated. However, studies using TRAP

Table 1. *Genes tested or mentioned in this study and their corresponding Log_2-fold changes*

TAIR ID	Gene name	TE DEX	TE Control	TRAP-seq (DTG)	RNA-seq (DEG)
AT2G18300	*HBI1*	–3.05 (0.12)	0.77 (1.70)	–5.26 (0.02)	ns
AT3G02260	*BIG*	–1.99 (0.25)	–2.92 (0.13)	1.07 (2.10)	ns
AT4G15130	*CCT2*	3.10 (8.57)	ns	3.01 (8.05)	ns
AT1G50030	*TOR*	–3.19 (0.11)	ns	ns	ns
AT5G10930	*CIPK5*	–3.83 (0.07)	1.23 (2.34)	–4.38 (0.05)	ns
AT3G09070	*OPS*	+inf	ns	1.44 (2.71)	–inf
AT1G60000	Unknown	–4.37 (0.05)	ns	–3.6 (0.08)	ns
AT3G23900	Unknown	–2.84 (0.14)	ns	–1.1 (0.46)	ns
AT4G21020	*LEA*	+inf	–inf	+inf	–inf
AT1G56570	*PGN*	–inf	ns	–inf	ns
AT4G34410	*RRTF1*	1.73 (3.32)	ns	7.78 (219.80)	ns
AT1G07280	Unknown	–4.49 (0.04)	ns	–4.45 (0.04)	ns
AT1G07900	*LBD1*	–inf	+inf	–inf	+inf
AT5G14740	*CA2*	–2.35 (0.20)	–0.94 (0.52)	–2.19 (0.22)	ns
AT3G16640	*TCTP*	ns	–1.43 (0.37)	0.84 (1.79)	ns
AT4G36990	*TBF1*	ns	ns	4.95 (30.91)	5.79 (55.33)
AT1G75830	*LCR67*	+inf	–inf	+inf	ns

TE, $Log_2(FPKM_{TRAP}/FPKM_{RNA})$; (*x*), absolute fold-change ($FPKM_{TRAP}/FPKM_{RNA}$); ns, not significant; +inf, denominator is not detected; –inf, numerator is not detected.

and ribosome footprinting have shown that the two methods identify similar sets of regulated transcripts during hypoxia in plants (Juntawong *et al.*, 2014), indicating that TRAP-seq is a robust method for identifying translationally regulated transcripts. Some of these changes could be induced by AvrRpm1, which could not be tested as discussed above. However, previous studies suggest that, at early time-points, AvrRpm1 has no effect on the transcriptional response to defense signaling independent of RPM1 (de Torres *et al.*, 2003). Given that the transcriptional response in our experimental system strongly resembles the expected transcriptional response of NB-LRR activation, it is reasonable assume that the vast majority of the translational responses, and the overall pattern of regulation, are attributable to NB-LRR activation. Most importantly, we have validated the involvement of a number of genes identified herein by showing their involvement in plant defenses against pathogens. Indeed, although the number of examples are limited for the time, translational up- and down-regulation correlated with positive and negative contributions to defense, suggesting that these responses are induced by NB-LRR signaling. These genes are involved in both ETI and PTI (Fig. 5) and thus, like transcriptional changes, translationally regulated transcripts may be involved in both types of resistance.

The TOR protein appears to be required for the translation of certain viral RNAs (Schepetilnikov *et al.*, 2011; Ouibrahim *et al.*, 2015). In addition to this, our results suggest an important role (or roles) for TOR in immunity as its TE is reduced approximately 10-fold ($Log_2 = –3.1$) upon NB-LRR activation (Table 1, Fig. 4D). Previous studies in Arabidopsis have characterized the transcriptome and the metabolome profiles in conditions of decreased TOR activity, either by chemical inhibition or by inhibiting TOR expression using RNAi. These studies showed that TOR reduction leads to a metabolic switch resulting in reduced anabolic activities, such as photosynthesis, and an increase in catabolism (Ren *et al.*, 2012; Caldana *et al.*, 2013). Plant defense responses result in a similar metabolic reprogramming, presumably because these responses are energetically demanding (Rojas *et al.*, 2014). Our datasets cannot be directly compared to all of these studies due to differences in experimental design, although the transcriptome of TOR-inhibited plants is significantly enriched in immune-related genes (see Supplementary Fig. S4). However, the similarity in metabolic switches suggests that NB-LRR activation induces a reorientation of cellular activities that allows the cell to generate energy and use it for defense-related responses, in part by down-regulating TOR activity. Thus, we suggest that TOR RNAi plants are more resistant to avirulent and virulent *Pst* and *Hpa* (Fig. 5) because lower TOR levels allow the plant cell to more rapidly switch from a growth to defense program. In contrast, TOR OX plants are more susceptible to virulent *Hpa* (Fig. 5D, F) due to a less efficient switch. Although we did not see increased susceptibility to *Pst* in the TOR OX lines, it has been reported that the Cauliflower Mosaic Virus P6 protein, which strongly activates TOR, causes increased susceptibility to *Pst* (Zvereva *et al.*, 2016). Thus, the differences seen between the two pathosystems with respect to the TOR OX line may be due to differences in thresholds. Further work will be required to determine whether TOR regulates immunity by regulating the translation of proteins involved in defense, and/or whether it contributes more broadly by altering the metabolic state of the cell. Alternatively, or in parallel, down-regulation of TOR contributes to defense through its role in suppressing autophagy (Liu and Bassham, 2010), which has been implicated in plant immunity (Hofius *et al.*, 2011; Zvereva *et al.*, 2016).

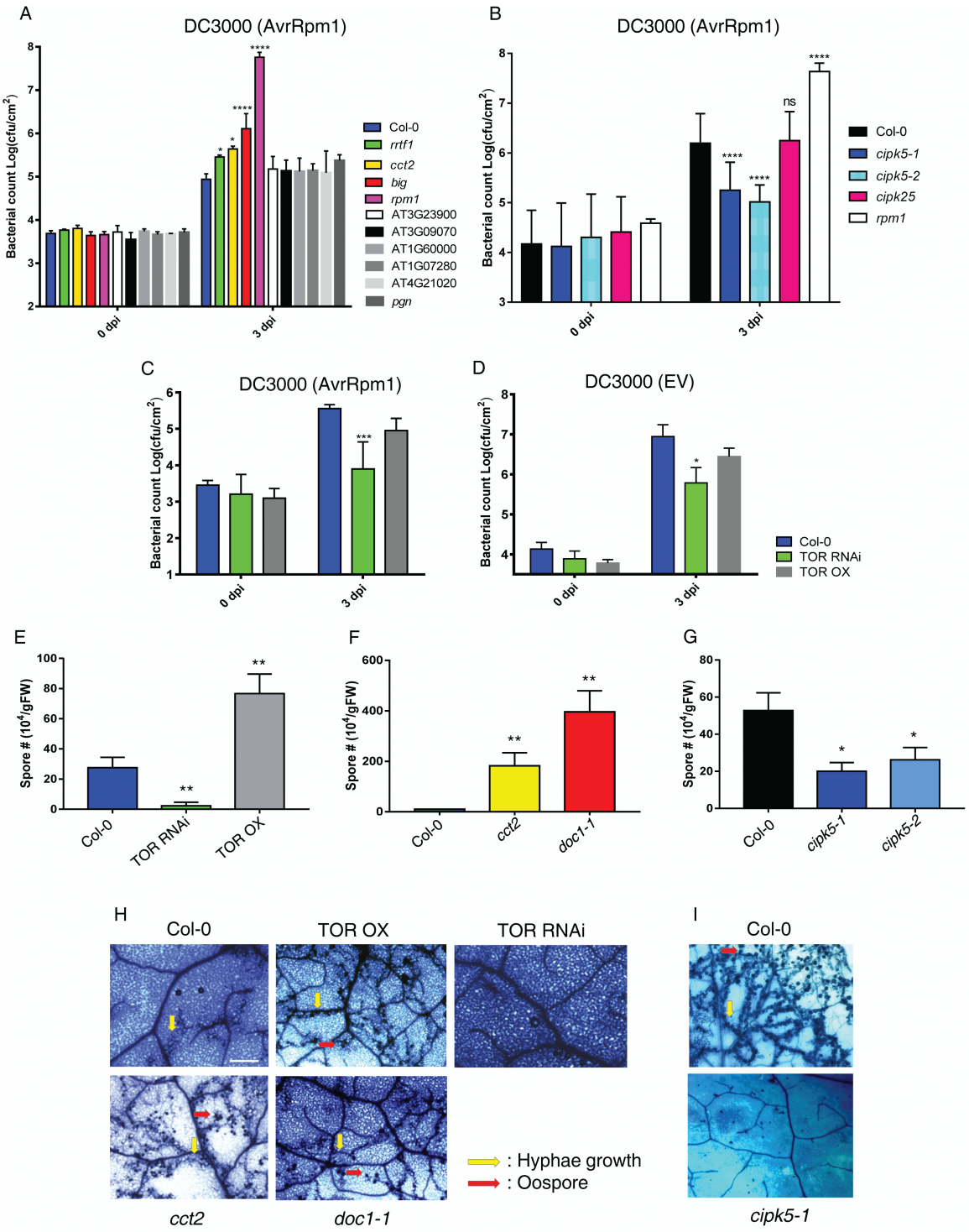

Fig. 5. Candidate gene validation. (A) Corresponding mutants of selected translationally regulated genes during defense were challenged with *Pseudomonas syringae* DC3000 (AvrRpm1). The graph indicates bacterial counts at 0 and 3 d post-infection (dpi) on a Log_{10} scale. Mean values (±SEM) were calculated for three independent biological replicates. Statistically significant differences were determined using two-way ANOVA and Holm–Sidak's multiple comparison test with Col-0 as a control: **P*<0.05, ***P*<0.01, ****P*<0.001, *****P*<0.0001). (B) Col-0, *cipk5-1*, *cipk5-2*, and *cipk25* mutant lines were infected and analysed as in (A). (C) Col-0, TOR RNAi, and TOR OX plants were infected and analysed as in (A). (D) Same as (C) but with *Pseudomonas syringae* DC3000 carrying an empty vector (EV) instead of AvrRpm1. (E– G) Spore numbers counted on the indicated plant lines infected with *Hyaloperonospora arabidopsidis* (Hpa) strain Noco2, 12 d after inoculation. Data are the mean (±SEM; $n = 3$). Significant differences were detected between mutant/transgenic plants and Col-0 using non-parametric Kruskal–Wallis and Dunn's multiple comparison tests: **P*<0.05, ***P*<0.01. (H, I) Trypan Blue staining of infected leaves, revealing hyphae and oospores from the indicated infected plants 12 d after infection with *Hpa* strain Noco2. Scale bar =250 μm.

Although the signaling pathways regulating TOR activity are not as well defined in plants as in other systems, it is interesting to note that our study has identified CBL-interacting protein kinase 5 (CIPK5) as an important regulator of defense. This protein, also known as SNF1-related protein kinase 3.24 (SnRK3.24), is part of a large family SNF1-related kinases,

including SnRK1, SnRK2, and SnRK3 proteins. SnRK1 proteins are most closely related to the SNF1 and AMPK kinases that negatively regulate TOR activity in yeast and mammals, respectively, while several SnRK2 and SnRK3 proteins have been shown to be important in the responses to different abiotic stresses (Hrabak *et al.*, 2003; Kolukisaoglu *et al.*, 2004; Crozet *et al.*, 2014). Interestingly, *CIPK5* transcripts are less abundant after prolonged TOR inhibition in Arabidopsis (Dong *et al.*, 2015). The *CIPK5* mRNA showed a decrease in TE upon DEX treatment, and ablation of this gene resulted in a more effective resistance response to both virulent and avirulent pathogens (Fig. 5). Thus, CIPK5 appears to be a negative regulator of defense that is down-regulated upon NB-LRR activation in order to permit a more effective growth-to-defense transition. It is interesting to speculate that CIPK5 might positively regulate TOR and that a lack of this activity in the *cipk5* mutant results in decreased TOR activity, leading to a more efficient growth-to-defense transition, similar to the TOR RNAi line.

The importance of a switch from growth to defense for resistance to pathogens has been inferred from a number of studies (Lozano-Durán and Zipfel, 2015). Notably, the HBI1 protein negatively regulates plant defenses. Knock-down of *HBI1* expression leads to decreased susceptibility to virulent *Pst* and HBI1 overexpression leads to increased susceptibility and increased growth (Fan *et al.*, 2014; Malinovsky *et al.*, 2014). Consistent with these reports, we found that the *HBI1* transcript had a significantly higher than average TE (Log_2 = 0.77) under normal conditions but that its translational status was 9-fold lower than expected (Log_2 = –3.05) upon activation of RPM1 (Fig. 3B). Thus, in addition to transcriptional down-regulation induced by PAMPs (Fan *et al.*, 2014; Malinovsky *et al.*, 2014), it would appear that NB-LRR signaling leads to a strong repression of HBI1 translation.

Our study also identified several genes not previously implicated in ETI or PTI responses, including *BIG* and *CCT2*, whose TEs increase upon NB-LRR activation (Fig. 5A, B). These mutants also showed increased susceptibility to *Hpa* (Fig. 5E, F), indicating that they are required for both NB-LRR and basal immunity. The *BIG* gene encodes a 5078-aa protein with multiple functional domains and has been implicated in several hormonal and light responses, possibly due to a role in endocytosis (Kanyuka *et al.*, 2003; Paciorek *et al.*, 2005). This function appears to result in a pronounced auxin-related phenotype (Gil *et al.*, 2001), which, given the antagonistic relationship between auxin and defense (Robert-Seilaniantz *et al.*, 2011), may contribute to the *big* defense phenotype. The CCT2 protein is involved in the production of phosphatidylcholine (Liao *et al.*, 2014) and its role in defense remains to be elucidated.

The mechanisms of translational status regulation by NB-LRR signaling are probably diverse, given the number of transcripts affected and the instances of both positive and negative regulation. Nonetheless, we have shown that some of the most strongly regulated genes are involved in pathogen defense, indicating that this approach is an effective method for identifying new players in plant immunity. Our results suggest that certain proteins (*BIG*, *CCT2*, *RRTF1*) are rapidly up-regulated at the translational level because they are required for disease resistance. Conversely, other transcripts (*HBI1*, *TOR*, *CIPK5*) show decreased TE upon RPM1 activation because their encoded proteins are normally suppressors of defense and/or promoters of growth. Future studies on the involvement of additional candidates, as well as the mechanisms by which they are regulated, will lead to a greater understanding of how plants defend themselves against pathogens and help to clarify the general mechanisms of translational control in plants.

Supplementary data

Fig. S1. Translating ribosome affinity purification (TRAP) followed by sequencing (TRAP-seq) quality controls.

Fig. S2. Technical features of RNA-seq and TRAP-seq libraries and protein domain enrichment analysis.

Fig. S3. Read accumulation of the TBF1 transcript as an example of a transcriptionally and translationally induced gene after DEX treatment.

Fig. S4. TOR inhibition leads to increased abundance of defense-related transcripts.

Table S1. List of genes with significantly increased or decreased abundance at the level of total RNA (DEGs) after DEX treatment.

Table S2. List of genes with significantly increased or decreased abundance on ribosomes after DEX treatment (DTGs).

Table S3. GO term enrichment analysis of DEGs and DTGs.

Table S4. List of significant (FDR<0.05) control, DEX, and common GUTTs.

Table S5. List of significant (FDR<0.05) common and defense GUTTs with their associated TE differentials upon DEX treatment.

Table S6. Raw Cuffdiff output of the systematic analysis allowing the identification of translationally regulated genes.

Supplementary Experimental Procedures. Details of the RT-PCR experiment, the sucrose cushion concentration and sucrose gradient fractionation, and immune-blotting and silver staining.

Acknowledgments

We are grateful to Christophe Robaglia for sharing the RNAi 35–7 TOR line, to Christian Meyer for the G548 TOR OX line, to Philippe Reymond for the *rrtf1* mutant and to David Mackey for the DEX:AvrRpm1 transgenics. We are particularly grateful to Julia Bailey-Serres for the FLAG-rpL18 transgenic plants and for technical advice and helpful discussions. This work was supported by funding from the National Science and Engineering Council of Canada (NSERC).

References

Caldana C, Li Y, Leisse A, Zhang Y, Bartholomaeus L, Fernie AR, Willmitzer L, Giavalisco P. 2013. Systemic analysis of inducible target of rapamycin mutants reveal a general metabolic switch controlling growth in *Arabidopsis thaliana*. The Plant Journal **73,** 897–909.

Carraro N, Matteau D, Luo P, Rodrigue S, Burrus V. 2014. The master activator of IncA/C conjugative plasmids stimulates genomic islands and multidrug resistance dissemination. PLoS Genetics **10,** e1004714.

Coate JE, Bar H, Doyle JJ. 2014. Extensive translational regulation of gene expression in an allopolyploid (*Glycine dolichocarpa*). The Plant Cell **26,** 136–150.

Coll NS, Epple P, Dangl JL. 2011. Programmed cell death in the plant immune system. Cell Death and Differentiation **18,** 1247–1256.

Crozet P, Margalha L, Confraria A, Rodrigues A, Martinho C, Adamo M, Elias CA, Baena-González E. 2014. Mechanisms of regulation of SNF1/AMPK/SnRK1 protein kinases. Frontiers in Plant Science **5,** 190.

de Torres M, Sanchez P, Fernandez-Delmond I, Grant M. 2003. Expression profiling of the host response to bacterial infection: the transition from basal to induced defence responses in RPM1-mediated resistance. The Plant Journal **33,** 665–676.

Deprost D, Yao L, Sormani R, Moreau M, Leterreux G, Nicolaï M, Bedu M, Robaglia C, Meyer C. 2007. The *Arabidopsis* TOR kinase links plant growth, yield, stress resistance and mRNA translation. EMBO Reports **8,** 864–870.

Dobrenel T, Caldana C, Hanson J, Robaglia C, Vincentz M, Veit B, Meyer C. 2016. TOR signaling and nutrient sensing. Annual Review of Plant Biology **67,** 261–285.

Dong P, Xiong F, Que Y, Wang K, Yu L, Li Z, Ren M. 2015. Expression profiling and functional analysis reveals that TOR is a key player in regulating photosynthesis and phytohormone signaling pathways in *Arabidopsis*. Frontiers in Plant Science **6,** 677.

Edgar R, Domrachev M, Lash AE. 2002. Gene expression omnibus: NCBI gene expression and hybridization array data repository. Nucleic Acids Research **30,** 207–210.

Fan M, Bai MY, Kim JG, *et al*. 2014. The bHLH transcription factor HBI1 mediates the trade-off between growth and pathogen-associated molecular pattern-triggered immunity in Arabidopsis. The Plant Cell **26,** 828–841.

Geng X, Mackey D. 2011. Dose–response to and systemic movement of dexamethasone in the GVG-inducible transgene system in *Arabidopsis*. Methods in Molecular Biology **712,** 59–68.

Geng X, Shen M, Kim JH, Mackey D. 2016. The *Pseudomonas syringae* type III effectors AvrRpm1 and AvrRpt2 promote virulence dependent on the F-box protein COI1. Plant Cell Reports **35,** 921–932.

Gil P, Dewey E, Friml J, Zhao Y, Snowden KC, Putterill J, Palme K, Estelle M, Chory J. 2001. BIG: a calossin-like protein required for polar auxin transport in Arabidopsis. Genes & Development **15,** 1985–1997.

González-Lamothe R, El Oirdi M, Brisson N, Bouarab K. 2012. The conjugated auxin indole-3-acetic acid–aspartic acid promotes plant disease development. The Plant Cell **24,** 762–777.

Hofius D, Munch D, Bressendorff S, Mundy J, Petersen M. 2011. Role of autophagy in disease resistance and hypersensitive response-associated cell death. Cell Death and Differentiation **18,** 1257–1262.

Hrabak EM, Chan CW, Gribskov M, *et al*. 2003. The *Arabidopsis* CDPK-SnRK superfamily of protein kinases. Plant Physiology **132,** 666–680.

Huang DW, Sherman BT, Lempicki RA. 2009. Systematic and integrative analysis of large gene lists using DAVID bioinformatics resources. Nature Protocols **4,** 44–57.

Jones AM, Thomas V, Bennett MH, Mansfield J, Grant M. 2006. Modifications to the Arabidopsis defense proteome occur prior to significant transcriptional change in response to inoculation with *Pseudomonas syringae*. Plant Physiology **142,** 1603–1620.

Jones AM, Thomas V, Truman B, Lilley K, Mansfield J, Grant M. 2004. Specific changes in the *Arabidopsis* proteome in response to bacterial challenge: differentiating basal and *R*-gene mediated resistance. Phytochemistry **65,** 1805–1816.

Joshi A, Van de Peer Y, Michoel T. 2011. Structural and functional organization of RNA regulons in the post-transcriptional regulatory network of yeast. Nucleic Acids Research **39,** 9108–9117.

Juntawong P, Bailey-Serres J. 2012. Dynamic light regulation of translation status in *Arabidopsis thaliana*. Frontiers in Plant Science **3,** 66.

Juntawong P, Girke T, Bazin J, Bailey-Serres J. 2014. Translational dynamics revealed by genome-wide profiling of ribosome footprints in *Arabidopsis*. Proceedings of the National Acadamy of Sciences, USA **111,** E203–212.

Kang HG, Fang Y, Singh KB. 1999. A glucocorticoid-inducible transcription system causes severe growth defects in *Arabidopsis* and induces defense-related genes. The Plant Journal **20,** 127–133.

Kanyuka K, Praekelt U, Franklin KA, Billingham OE, Hooley R, Whitelam GC, Halliday KJ. 2003. Mutations in the huge *Arabidopsis* gene *BIG* affect a range of hormone and light responses. The Plant Journal **35,** 57–70.

Keene JD. 2007. RNA regulons: coordination of post-transcriptional events. Nature Reviews Genetics **8,** 533–543.

Kim D, Pertea G, Trapnell C, Pimentel H, Kelley R, Salzberg SL. 2013. TopHat2: accurate alignment of transcriptomes in the presence of insertions, deletions and gene fusions. Genome Biology **14,** R36.

Kolukisaoglu U, Weinl S, Blazevic D, Batistic O, Kudla J. 2004. Calcium sensors and their interacting protein kinases: genomics of the *Arabidopsis* and rice CBL-CIPK signaling networks. Plant Physiology **134,** 43–58.

Laluk K, Abuqamar S, Mengiste T. 2011. The *Arabidopsis* mitochondria-localized pentatricopeptide repeat protein PGN functions in defense against necrotrophic fungi and abiotic stress tolerance. Plant Physiology **156,** 2053–2068.

Langmead B, Salzberg SL. 2012. Fast gapped-read alignment with Bowtie 2. Nature Methods **9,** 357–359.

Li H, Handsaker B, Wysoker A, Fennell T, Ruan J, Homer N, Marth G, Abecasis G, Durbin R(1000 Genome Project Data Processing Subgroup). 2009. The Sequence Alignment/Map format and SAMtools. Bioinformatics **25,** 2078–2079.

Li X, Kapos P, Zhang Y. 2015. NLRs in plants. Current Opinion in Immunology **32,** 114–121.

Liao P, Chen QF, Chye ML. 2014. Transgenic *Arabidopsis* flowers overexpressing acyl-CoA-binding protein ACBP6 are freezing tolerant. Plant & Cell Physiology **55,** 1055–1071.

Lin SY, Chen PW, Chuang MH, Juntawong P, Bailey-Serres J, Jauh GY. 2014. Profiling of translatomes of *in vivo*-grown pollen tubes reveals genes with roles in micropylar guidance during pollination in *Arabidopsis*. The Plant Cell **26,** 602–618.

Liu MJ, Wu SH, Wu JF, Lin WD, Wu YC, Tsai TY, Tsai HL, Wu SH. 2013. Translational landscape of photomorphogenic *Arabidopsis*. The Plant Cell **25,** 3699–3710.

Liu MJ, Wu SH, Chen HM, Wu SH. 2012. Widespread translational control contributes to the regulation of *Arabidopsis* photomorphogenesis. Molecular Systems Biology **8,** 566.

Liu Y, Bassham DC. 2010. TOR is a negative regulator of autophagy in *Arabidopsis thaliana*. PLoS ONE **5,** e11883.

Lozano-Durán R, Zipfel C. 2015. Trade-off between growth and immunity: role of brassinosteroids. Trends in Plant Science **20,** 12–19.

Macho AP, Zipfel C. 2014. Plant PRRs and the activation of innate immune signaling. Molecular Cell **54,** 263–272.

Macho AP, Zipfel C. 2015. Targeting of plant pattern recognition receptor-triggered immunity by bacterial type-III secretion system effectors. Current Opinion in Microbiology **23,** 14–22.

Mackey D, Holt BF III, Wiig A, Dangl JL. 2002. RIN4 interacts with *Pseudomonas syringae* type III effector molecules and is required for RPM1-mediated resistance in Arabidopsis. Cell **108,** 743–754.

Malinovsky FG, Batoux M, Schwessinger B, Youn JH, Stransfeld L, Win J, Kim SK, Zipfel C. 2014. Antagonistic regulation of growth and immunity by the Arabidopsis basic helix-loop-helix transcription factor homolog of brassinosteroid enhanced expression2 interacting with increased leaf inclination1 binding bHLH1. Plant Physiology **164,** 1443–1455.

Menand B, Desnos T, Nussaume L, Berger F, Bouchez D, Meyer C, Robaglia C. 2002. Expression and disruption of the *Arabidopsis TOR* (target of rapamycin) gene. Proceedings of the National Acadamy of Sciences, USA **99,** 6422–6427.

Meteignier LV, Zhou J, Cohen M, Bhattacharjee S, Brosseau C, Chan MG, Robatzek S, Moffett P. 2016. NB-LRR signaling induces translational repression of viral transcripts and the formation of RNA processing bodies through mechanisms differing from those activated by UV stress and RNAi. Journal of Experimental Botany **67,** 2353–2366.

Moeller JR, Moscou MJ, Bancroft T, Skadsen RW, Wise RP, Whitham SA. 2012. Differential accumulation of host mRNAs on

polyribosomes during obligate pathogen–plant interactions. Molecular Biosystems **8,** 2153–2165.

Mustroph A, Juntawong P, Bailey-Serres J. 2009. Isolation of plant polysomal mRNA by differential centrifugation and ribosome immunopurification methods. Methods in Molecular Biology **553,** 109–126.

Navarro L, Zipfel C, Rowland O, Keller I, Robatzek S, Boller T, Jones JD. 2004. The transcriptional innate immune response to flg22. Interplay and overlap with Avr gene-dependent defense responses and bacterial pathogenesis. Plant Physiology **135,** 1113–1128.

Ouibrahim L, Rubio AG, Moretti A, Montané MH, Menand B, Meyer C, Robaglia C, Caranta C. 2015. Potyviruses differ in their requirement for TOR signalling. The Journal of General Virology **96,** 2898–2903.

Paciorek T, Zazímalová E, Ruthardt N, *et al*. 2005. Auxin inhibits endocytosis and promotes its own efflux from cells. Nature **435,** 1251–1256.

Pajerowska-Mukhtar KM, Wang W, Tada Y, Oka N, Tucker CL, Fonseca JP, Dong X. 2012. The HSF-like transcription factor TBF1 is a major molecular switch for plant growth-to-defense transition. Current Biology **22,** 103–112.

Ren M, Venglat P, Qiu S, *et al*. 2012. Target of rapamycin signaling regulates metabolism, growth, and life span in *Arabidopsis*. The Plant Cell **24,** 4850–4874.

Reynoso MA, Juntawong P, Lancia M, Blanco FA, Bailey-Serres J. 2015. Microgenomics: genome-scale, cell-specific monitoring of multiple gene regulation tiers. Methods in Molecular Biology **1284,** 185–207.

Robert-Seilaniantz A, Grant M, Jones JD. 2011. Hormone crosstalk in plant disease and defense: more than just jasmonate-salicylate antagonism. Annual Review of Phytopathology **49,** 317–343.

Rojas CM, Senthil-Kumar M, Tzin V, Mysore KS. 2014. Regulation of primary plant metabolism during plant–pathogen interactions and its contribution to plant defense. Frontiers in Plant Science **5,** 17.

Schepetilnikov M, Kobayashi K, Geldreich A, Caranta C, Robaglia C, Keller M, Ryabova LA. 2011. Viral factor TAV recruits TOR/S6K1 signalling to activate reinitiation after long ORF translation. The EMBO Journal **30,** 1343–1356.

Schweizer F, Bodenhausen N, Lassueur S, Masclaux FG, Reymond P. 2013. Differential contribution of transcription Factors to *Arabidopsis thaliana* defense against *Spodoptera littoralis*. Frontiers in Plant Science **4,** 13.

Tao Y, Xie Z, Chen W, Glazebrook J, Chang HS, Han B, Zhu T, Zou G, Katagiri F. 2003. Quantitative nature of Arabidopsis responses during compatible and incompatible interactions with the bacterial pathogen *Pseudomonas syringae*. The Plant Cell **15,** 317–330.

Trapnell C, Hendrickson DG, Sauvageau M, Goff L, Rinn JL, Pachter L. 2013. Differential analysis of gene regulation at transcript resolution with RNA-seq. Nature Biotechnology **31,** 46–53.

Trapnell C, Pachter L, Salzberg SL. 2009. TopHat: discovering splice junctions with RNA-Seq. Bioinformatics **25,** 1105–1111.

Trapnell C, Williams BA, Pertea G, Mortazavi A, Kwan G, van Baren MJ, Salzberg SL, Wold BJ, Pachter L. 2010. Transcript assembly and quantification by RNA-Seq reveals unannotated transcripts and isoform switching during cell differentiation. Nature Biotechnology **28,** 511–515.

Tsuda K, Katagiri F. 2010. Comparing signaling mechanisms engaged in pattern-triggered and effector-triggered immunity. Current Opinion in Plant Biology **13,** 459–465.

Vragovic K, Sela A, Friedlander-Shani L, Fridman Y, Hacham Y, Holland N, Bartom E, Mockler TC, Savaldi-Goldstein S. 2015. Translatome analyses capture of opposing tissue-specific brassinosteroid signals orchestrating root meristem differentiation. Proceedings of the National Academy of Sciences, USA **112,** 923–928.

Xiong Y, McCormack M, Li L, Hall Q, Xiang C, Sheen J. 2013. Glucose-TOR signalling reprograms the transcriptome and activates meristems. Nature **496,** 181–186.

Yángüez E, Castro-Sanz AB, Fernández-Bautista N, Oliveros JC, Castellano MM. 2013. Analysis of genome-wide changes in the translatome of *Arabidopsis* seedlings subjected to heat stress. PLoS ONE **8,** e71425.

Yoshioka K, Moeder W, Kang HG, Kachroo P, Masmoudi K, Berkowitz G, Klessig DF. 2006. The chimeric Arabidopsis CYCLIC NUCLEOTIDE-GATED ION CHANNEL11/12 activates multiple pathogen resistance responses. The Plant Cell **18,** 747–763.

Zanetti ME, Chang IF, Gong F, Galbraith DW, Bailey-Serres J. 2005. Immunopurification of polyribosomal complexes of *Arabidopsis* for global analysis of gene expression. Plant Physiology **138,** 624–635.

Zvereva AS, Golyaev V, Turco S, *et al*. 2016. Viral protein suppresses oxidative burst and salicylic acid-dependent autophagy and facilitates bacterial growth on virus-infected plants. The New Phytologist **211,** 1020–1034.